ISSN: 2584-0231(Online)
International Journal of Multidisciplinary Research in Arts, Science and Technology
© IJMRAST \ Vol. 1 \ Issue 5 \ December 2023
Available online at: https://ijmrast.com
DOI: https://doi.org/10.61778/ijmrast.v1i5.29

Investigation via simulation of the influence of defects on the photovoltaic performance of single-junction perovskite solar cells based on $MAPbI_3$ using SCAPS-1D

Prem Pratap Singh and Kripa Shanker Singh

Department of Physics, RBS College, Dr. Bhimrao Ambedkar University, Agra-282002 UP India

***Corresponding Author:** mr.prem@live.com

ABSTRACT

This communication presents a numerical simulation study conducted on Perovskite Solar Cells (PSCs) featuring $MAPbI_3$ as the light-absorbing layer, utilizing the Solar Cell Capacitance Simulator (SCAPS-1D) software. The present study focuses on a single-junction solar cell architecture comprising TiO_2/$MAPbI_3$/Spiro-OMeTAD. SCAPS was employed to simulate how changes in the thickness of the absorber layer and the concentration of charges and defects within the absorber material affect the photovoltaic performance parameters of PSCs. The straightforward architecture of the solar cell has streamlined the investigation and optimization of device parameters. The 1D optimization of the PSC proposed in this study has led to optimized thickness of active layers, as well as the concentration of charges and defects within the $MAPbI_3$ absorber material. The present research work reports an optimum thickness of 450 nm for $MAPbI_3$ absorber material. The optimized concentration of defects has been found to be 10^{14} cm^{-1}. The defect charge type in the absorber layer has not been found to affect the photovoltaic parameters of the PSC.

Keywords: *Perovskite solar cells, $MAPbI_3$, Defects, SCAPS-1D*

1. Introduction

Hybrid organic-inorganic perovskite solar cells (PSCs) have garnered global interest due to their excellent characteristics, comprising a high coefficient of absorption, elevated carrier mobility, extended carrier lifetime, and straightforward fabrication process [1-5]. The standard formula for perovskites is represented as ABX_3, where A stands for an organic methylammonium ($CH_3NH_3^+$) ion [6] or formamidinium ($NH{=}CHNH_3^+$) ion [7-9], B represents an inorganic cation such as Pb^{2+} or Sn^{2+}, and X denotes a halogen ion, typically I^-, Br^-, or Cl^-. Among various combinations, the prevalent halide perovskite is methylammonium lead iodide ($MAPbI_3$) [10]. In 2009, Kojima and co-workers reported the first PSC [11]. Solid sensitizers used by them in dye-sensitized solar cells (DSSCs) having liquid electrolyte

comprised methylammonium lead iodide ($CH_3NH_3PbI_3$, '$MAPbI_3$') and methylammonium lead bromide ($CH_3NH_3PbBr_3$, '$MAPbBr_3$').

Despite rapid advances, some material properties that are critical to photovoltaic performance are still poorly understood. Comprehending the origins of the various features of ABX_3 materials could be a crucial step in the adoption of perovskites-based photovoltaics on a broad scale. In this context, a computational technique capable of accurately estimating various material properties, allowing for the design of new materials and the interpretation of their qualities, is essential. Various studies on perovskite solar cells utilising SCAPS are reported in the literature [12-15]. Abdelaziz et al. [16] (2020) used SCAPS device modelling to study the photovoltaic performance parameters of a formamidinium tin-based PSC, reporting a PCE of 14.03 %. Raoui et al. (2019) examined the $MAPbI_3$-based perovskite solar cell performance using a range of charge selective contacts.

Many features of perovskite materials are still unknown. Three uncommon findings in particular have attracted great attention: (i) the slow electrical response of the material when exposed to light [17,18]; (ii) the anomalous hysteresis behaviour of the current–voltage (J–V) curves displayed by several PSC based devices [19–24]; and (iii) recent reports on giant switchable PV device [25, 26]. The most widely used hypotheses to explain the features of PSCs are: (i) charge trapping [27-30], (ii) ferroelectricity [31-34], and (iii) ion/defect migration or conductivity. Deep defects at the band gap center become more difficult to deal with because they trap both kinds of carriers, giving charge transport recombination plenty of time [35-37]. The energies of transition-state of all recognized typical point traps in $MAPbI_3$ complex were examined by Yin et al., who also found evidence of shallow-level defects and deep-level defects in the bandgap [38]. Space-charge-limited current measurements [39] were used to identify shallow defects, which had a density of about 10^{10}–10^{11} cm^{-3}. On the other hand, deep defects, which had a density of 10^{14}–10^{16} cm^{-3}, were characterized by means of time-resolved photoluminescence [40], transient photocurrent measurements [41], and deep-level transient spectroscopy [42]. Irrespective of the processing method used, Sung Heo et al. [42] detected two types of deep defect concentrations at energies below the conduction band edge at 0.65 eV (E_1) and 0.76 eV (E_2) in their perovskite solar cells that were created using both one-pot and cuboid procedures.

Utilizing the SCAPS-1D solar cell simulation software, we present simulations of single-junction $MAPbI_3$ solar photovoltaic cells. The aim of this study is to enhance comprehension of lead halide-based PSC performance by investigating the effect of thickness of the light absorbing layer, density of defects, and charge type on photovoltaic performance of the device. Additionally, the modeling outcomes could offer valuable understandings for the design and fabrication of forthcoming lead halide-based PSCs.

2. Simulation Methodology

In the current study, we employed the Solar Cell Capacitance Simulator (SCAPS) version 3.3.10 (ELIS, University of Gent, Belgium) as our simulation platform. This software operates on the three coupled differential equations: (1) Poisson's Equation, (2) Continuity equation for holes, (3) Continuity equation for electrons [43-46]:

$$\frac{d}{dx}\left(\varepsilon(x)\frac{d\Psi}{dx}\right) = q[p(x) - n(x) + N_D^+(x) - N_A^-(x) + p_t(x) - n_t(x)] \quad (1)$$

$$\frac{1}{j}\frac{dJ_P}{dx} + R_p(x) - G(x) = 0 \quad (2)$$

$$-\frac{1}{j}\frac{dJ_n}{dx} + R_n(x) - G(x) = 0 \quad (3)$$

Here, ε represents the permittivity, electron charge is denoted by q, ψ gives the electrostatic potential and n and p represent the concentration of electrons and that of free holes respectively, trapped electrons is given by n_t while p_t gives trapped hole, concentrations of ionized donor-like doping is given by N_D^+ and concentration of ionized acceptor-like doping is given by N_A^-, $R_n(x)$, $R_p(x)$ are the rates of recombination for electrons and holes, G(x) gives the rate of generation, J_n and J_p show the current densities for electron and hole respectively. It has been applied to simulation research on several solar cell types [47-52].

In this simulation work single junction planar structure has been considered, in which the transparent n-type metal oxide semi-conductor was modelled by using ETM TiO_2, $CH_3NH_3PbI_3$ as light harvesting material, and Spiro-OMeTAD has been used as hole transport material (Fig. 1). Table 1 lists the values of the input parameters for simulation taken into account in SCAPS-1D, which were taken from theory and reported in literature [53-67].

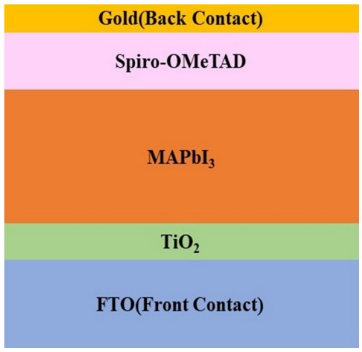

Figure 1: Schematic of the perovskite solar cell structure simulated in the present study.

Table 1: Parameters used for simulation of the perovskite solar cell [53-67]

Parameter	**n-TiO_2**	**$MAPbI_3$**	**Spiro-OMeTAD**
Thickness (nm)	90	450	Wide-range
Eg (eV)	3.2	3.2	2.9
χ (ev)	4	4	2.2
Ɛr	100	100	3
Nc ($1/cm^3$)	1×10^{21}	1×10^{21}	2.5×10^{20}
Nv ($1/cm^3$)	2×10^{20}	2×10^{20}	2.5×10^{20}
μn (cm^2/Vs)	0.006	0.006	0.0021
μp (cm^2/Vs)	0.006	0.006	0.0026
NA ($1/cm^3$)	-	-	1×10^{18}
ND ($1/cm^3$)	5.06×10^{19}	5.06×10^{19}	-

In the present device simulation of solar cell, interface defect layer (IDL) of TiO_2/$MAPbI_3$ and $MAPbI_3$/HTM have also been introduced. The Spiro-OMeTAD layer work function has been considered with respect to the energy level of the valence band and input parameters have been summarized in Table 2. AM 1.5G spectrum was used to obtain current density-voltage (J-V) curve under illumination.

Table 2: Interface layer parameters considered in the present study

Interface	**Type of Defect**	**Capture cross section electrons/holes (cm^2)**	**Energetic distribution**	**Reference for defect energy level E_t**	**Total density (integrated over all energies) ($1/cm^2$)**	**Total density (integrated over all energies) ($1/cm^2$)**
TiO_2/$MAPbI_3$	Acceptor	1×10^{-17}	Single	Above the VB	0.32	1×10^{9}
		1×10^{-18}		maximum		
$MAPbI_3$/Spiro-OMeTAD	Acceptor	1×10^{-18}	Single	Above the VB	0.07	1×10^{9} – 1×10^{12}
		1×10^{-19}		maximum		

3. Results and discussion

3.1. Influence of thickness of $MAPbI_3$ layer

For investigating the impact of one or more factors on solar cell properties, SCAPS provides a batch option. Users may pick the parameter to be adjusted, as well as the range and mode, in the 'Batch set-up' window. 'Batch set-up' allows for the definition of several parameters that may be adjusted simultaneously or in a hierarchical fashion.

In this work, we examined the effects of changing the thickness of light-absorbing $MAPbI_3$ layer on the Perovskite solar cells' photovoltaic performance characteristics. In ten-fold steps, the thickness of the absorber layer was changed from 0.1µm to 1µm. Figure 2 shows the PV parameters that were derived from the simulations. The efficiency of solar cells increases noticeably as the thickness of the absorber layer rises, as seen in Figure 2. But over 450 nm in thickness, the rate of efficiency enhancement decreases noticeably. As a result, we have tuned the light-absorbing Perovskite layer's thickness to be 450 nm.

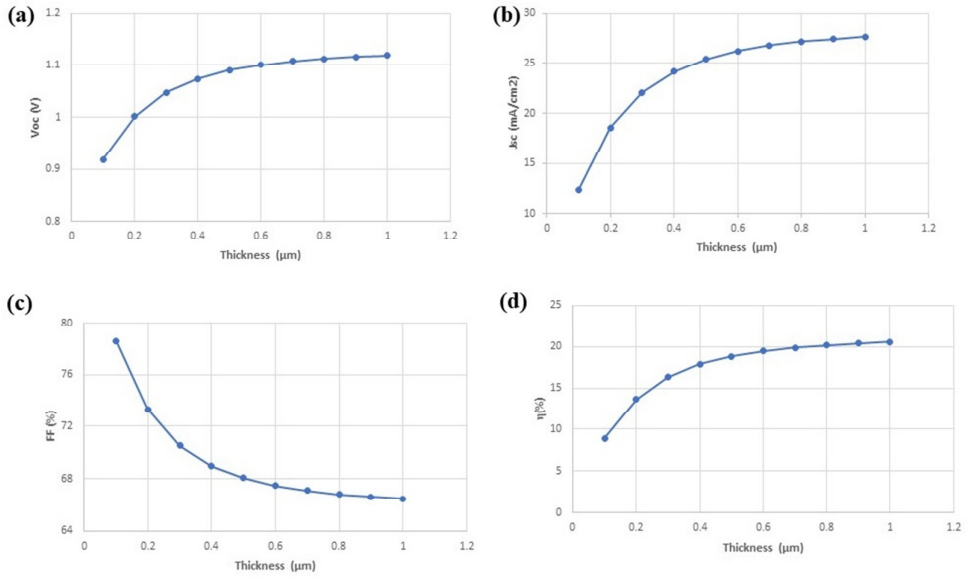

Figure 2: Variation of photovoltaic parameters with the thickness of the absorber perovskite layer of solar cells

3.2. Effect of defects in perovskite material on the device performance

Since photoelectrons are primarily produced and reassembled in the light absorbing layer, the density and kind of defects in perovskite material show a critical part in determining the photovoltaic performance of PSCs. Table 3 lists the various defect characteristics that were investigated in this simulation investigation. The effect of charge type and concentration of various flaws on the efficiency of PSCs is depicted in Fig. 3.

Table 3: Defect parameters used in the present simulation experiment

Type of Defect	DONOR/ NEUTRAL/ACCEPTOR
Electron Capture cross section (cm^2)	$1X\ 10^{-15}$
Hole Capture cross section (cm^2)	$1X\ 10^{-15}$
Energetic distribution	Single
Defect energy level Reference Et	Above EV of left side
Energy with respect to reference (eV)	0.600
Total density (1/cm^2)	$1\ X\ 10^{12}$ - $1\ X\ 10^{20}$

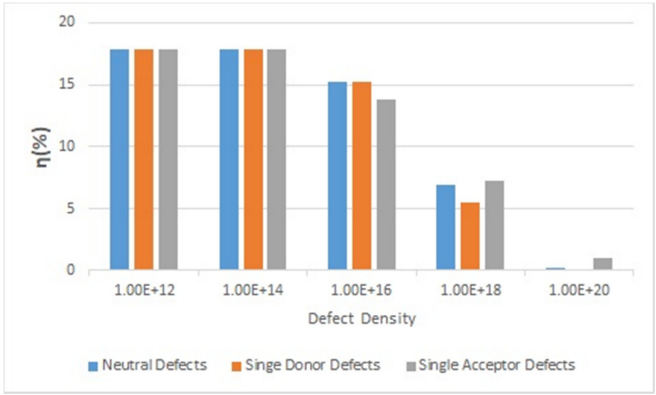

Figure 3: Effect of different defects charge type and concentration on the efficiency of perovskite solar cell.

The lifetime of minority charge carriers within the light-absorbing layer is dictated by the concentration of bulk defects [68]. Photovoltaic performance remains consistent until the defect density reaches 10^{14} cm^{-3}, regardless of the type of defects. It has been observed that when the density of defects within the light-absorbing layer is below 10^{14} cm^{-3}, efficiency does not exhibit significant variation. This could be owing to the fact that defect-photogenerated carrier scattering is less at lower densities of defects, and hence the solar cell device's performance remains unaffected. However, when the defect density is increased to high levels, the efficiency drops significantly. When the defects density is increased from 10^{14} to 10^{16} cm^{-3}, photovoltaic efficiency falls gradually at first, then rapidly. It's also worth noting that the defect charge type has little impact on the photovoltaic performance of the simulated perovskite solar cells.

Due of the material's low thermal stability, organohalide perovskites are susceptible to development of defects. Localized states could be introduced by surface imperfections of perovskite and at grain boundaries, which could trap photogenerated charge carriers and so produce a field across the material, ultimately counteracting the photogenerated potential.

The crystalline defects that serve as recombination centres have a significant impact on carrier dynamics and drastically reduce photoluminescence lifespan, resulting in device performance degradation [69-71]. Crystalline defects cause instability difficulties such as ion movement, hysteresis, and chemical degradation [72,73]. Therefore, to fully harness perovskite's promise for more competitive photovoltaic devices, defect management and mitigation are critical.

4. Conclusions

Using SCAPS-1D, simulations were conducted on single-junction perovskite solar cells with a TiO_2/$MAPbI_3$/Spiro-OMeTAD structure. The impact of the thickness of the absorber layer and the concentration and charge of defects on the photovoltaic performance was analyzed. It was found that the perovskite layer's thickness, with an ideal thickness of 450 nm, may be adjusted to maximize device performance. The study highlights the importance of maintaining defect concentrations in the absorber layer below 10^{14} cm^{-3} to achieve enhanced efficiency in perovskite solar cell designs. Additionally, further enhancements in perovskite-based solar cell performance can be attained by employing tandem geometries.

Acknowledgements

We extend our gratitude to Prof. M. Burgleman and his team at the University of Ghent, Belgium, for providing the SCAPS-1D software.

References

[1] Bi, D., Tress, W., Dar, M. I., Gao, P., Luo, J., Renevier, C., & Hagfeldt, A. (2016). Efficient luminescent solar cells based on tailored mixed-cation perovskites. *Science advances*, *2*(1), e1501170.

[2] Zhang, F., Wang, S., Li, X., & Xiao, Y. (2016). Recent progress of perovskite solar cells. *Curr. Nanosci*, *12*(2), 137-156.

[3] Kojima, A., Teshima, K., Shirai, Y., & Miyasaka, T. (2009). Organometal halide perovskites as visible-light sensitizers for photovoltaic cells. *Journal of the American Chemical Society*, *131*(17), 6050-6051.

[4] Xing, G., Mathews, N., Sun, S., Lim, S. S., Lam, Y. M., Grätzel, M., ... & Sum, T. C. (2013). Long-range balanced electron-and hole-transport lengths in organic-inorganic CH3NH3PbI3. *Science*, *342*(6156), 344-347.

[5] Bakr, Z. H., Wali, Q., Fakharuddin, A., Schmidt-Mende, L., Brown, T. M., & Jose, R. (2017). Advances in hole transport materials engineering for stable and efficient perovskite solar cells. *Nano Energy*, *34*, 271-305.

[6] Kazim, S., Nazeeruddin, M. K., Grätzel, M., & Ahmad, S. (2014). Perovskite as light harvester: a game changer in photovoltaics. *Angewandte Chemie International Edition*, *53*(11), 2812-2824.

[7] Eperon, G. E., Stranks, S. D., Menelaou, C., Johnston, M. B., Herz, L. M., & Snaith, H. J. (2014). Formamidinium lead trihalide: a broadly tunable perovskite for efficient planar heterojunction solar cells. *Energy & Environmental Science*, *7*(3), 982-988.

[8] Koh, T. M., Fu, K., Fang, Y., Chen, S., Sum, T. C., Mathews, N., ... & Baikie, T. (2014). Formamidinium-containing metal-halide: an alternative material for near-IR absorption perovskite solar cells. *The Journal of Physical Chemistry C*, *118*(30), 16458-16462.

[9] Salado, M., Kazim, S., Nazeeruddin, M. K., & Ahmad, S. (2019). Appraisement of Crystal Expansion in CH3NH3PbI3 on Doping: Improved Photovoltaic Properties. *ChemSusChem*, *12*(11), 2366-2372.

[10] Kearney K, Seo G, Matsushima T, Adachi C, Ertekin E, Rockett A. Computational Analysis of the Interplay between Deep Level Traps and Perovskite Solar Cell Efficiency. J Am Chem Soc 2018;140(46):15655–60.

[11] Kojima, A., Teshima, K., Shirai, Y., & Miyasaka, T. (2009). Organometal halide perovskites as visible-light sensitizers for photovoltaic cells. *Journal of the American Chemical Society*, *131*(17), 6050-6051.

[12] Abdelaziz, S., Zekry, A., Shaker, A., & Abouelatta, M. (2020). Investigating the performance of formamidinium tin-based perovskite solar cell by SCAPS device simulation. *Optical Materials*, *101*, 109738.

[13] Azri, F., Meftah, A., Sengouga, N., & Meftah, A. (2019). Electron and hole transport layers optimization by numerical simulation of a perovskite solar cell. *Solar energy*, *181*, 372-378.

[14] Haidari, G. (2019). Comparative 1D optoelectrical simulation of the perovskite solar cell. *AIP Advances*, *9*(8), 085028.

[15] Kuang, Y., Zardetto, V., van Gils, R., Karwal, S., Koushik, D., Verheijen, M. A., ... & Creatore, M. (2018). Low-temperature plasma-assisted atomic-layer-deposited SnO2 as an electron transport layer in planar Perovskite solar cells. *ACS applied materials & interfaces*, *10*(36), 30367-30378.

[16] Abdelaziz, S., Zekry, A., Shaker, A., & Abouelatta, M. (2020). Investigating the performance of formamidinium tin-based perovskite solar cell by SCAPS device simulation. *Optical Materials*, *101*, 109738.

[17] Gottesman, R., Haltzi, E., Gouda, L., Tirosh, S., Bouhadana, Y., Zaban, A., ... & De Angelis, F. (2014). Extremely slow photoconductivity response of CH3NH3PbI3 perovskites suggesting structural changes under working conditions. *The journal of physical chemistry letters*, *5*(15), 2662-2669.

[18] Juarez-Perez, E. J., Sanchez, R. S., Badia, L., Garcia-Belmonte, G., Kang, Y. S., Mora-Sero, I., & Bisquert, J. (2014). Photoinduced giant dielectric constant in lead halide perovskite solar cells. *The journal of physical chemistry letters*, *5*(13), 2390-2394.

[19] Snaith, H. J., Abate, A., Ball, J. M., Eperon, G. E., Leijtens, T., Noel, N. K., ... & Zhang, W. (2014). Anomalous hysteresis in perovskite solar cells. *The journal of physical chemistry letters*, *5*(9), 1511-1515.

[20] Chen, H. W., Sakai, N., Ikegami, M., & Miyasaka, T. (2015). Emergence of hysteresis and transient ferroelectric response in organo-lead halide perovskite solar cells. *The journal of physical chemistry letters*, *6*(1), 164-169.

[21] Tress, W., Marinova, N., Moehl, T., Zakeeruddin, S. M., Nazeeruddin, M. K., & Grätzel, M. (2015). Understanding the rate-dependent J–V hysteresis, slow time component, and aging in CH 3 NH 3 PbI 3 perovskite solar cells: the role of a compensated electric field. *Energy & Environmental Science*, *8*(3), 995-1004.

[22] Kim, H. S., & Park, N. G. (2014). Parameters affecting I–V hysteresis of CH3NH3PbI3 perovskite solar cells: effects of perovskite crystal size and mesoporous TiO2 layer. *The journal of physical chemistry letters*, *5*(17), 2927-2934.

[23] Unger, E. L., Hoke, E. T., Bailie, C. D., Nguyen, W. H., Bowring, A. R., Heumüller, T., & McGehee, M. D. (2014). Hysteresis and transient behavior in current–voltage measurements of hybrid-perovskite absorber solar cells. *Energy & Environmental Science*, *7*(11), 3690-3698.

[24] Chen, B., Zheng, X., Yang, M., Zhou, Y., Kundu, S., Shi, J., & Priya, S. (2015). Interface band structure engineering by ferroelectric polarization in perovskite solar cells. *Nano Energy*, *13*, 582-591.

[25] Park, N. G. (2015). Switchable photovoltaics. *Nature materials*, *14*(2), 140-141.

[26] Xiao, Z., Yuan, Y., Shao, Y., Wang, Q., Dong, Q., Bi, C., & Huang, J. (2015). Giant switchable photovoltaic effect in organometal trihalide perovskite devices. *Nature materials*, *14*(2), 193-198.

[27] Shao, Y., Xiao, Z., Bi, C., Yuan, Y., & Huang, J. (2014). Origin and elimination of photocurrent hysteresis by fullerene passivation in CH 3 NH 3 PbI 3 planar heterojunction solar cells. *Nature communications*, *5*(1), 1-7.

[28] Wojciechowski, K., Stranks, S. D., Abate, A., Sadoughi, G., Sadhanala, A., Kopidakis, N., ... & Snaith, H. J. (2014). Heterojunction modification for highly efficient organic–inorganic perovskite solar cells. *ACS nano*, *8*(12), 12701-12709.

[29] Xiao, Z., Bi, C., Shao, Y., Dong, Q., Wang, Q., Yuan, Y., & Huang, J. (2014). Efficient, high yield perovskite photovoltaic devices grown by interdiffusion of solution-processed precursor stacking layers. *Energy & Environmental Science*, *7*(8), 2619-2623.

[30] Nagaoka, H., Ma, F., Dequilettes, D. W., Vorpahl, S. M., Glaz, M. S., Colbert, A. E., ... & Ginger, D. S. (2015). Zr incorporation into TiO2 electrodes reduces hysteresis and improves performance in hybrid perovskite solar cells while increasing carrier lifetimes. *The journal of physical chemistry letters*, *6*(4), 669-675.

[31] Bertoluzzi, L., Sanchez, R. S., Liu, L., Lee, J. W., Mas-Marza, E., Han, H., ... & Bisquert, J. (2015). Cooperative kinetics of depolarization in CH 3 NH 3 PbI 3 perovskite solar cells. *Energy & Environmental Science*, *8*(3), 910-915.

[32] Frost, J. M., Butler, K. T., & Walsh, A. APL Mater. 2, 081506 (2014).

[33] Kutes, Y., Ye, L., Zhou, Y., Pang, S., Huey, B. D., & Padture, N. P. (2014). Direct observation of ferroelectric domains in solution-processed CH3NH3PbI3 perovskite thin films. *The journal of physical chemistry letters*, *5*(19), 3335-3339.

[34] Frost, J. M., Butler, K. T., Brivio, F., Hendon, C. H., Van Schilfgaarde, M., & Walsh, A. (2014). Atomistic origins of high-performance in hybrid halide perovskite solar cells. *Nano letters*, *14*(5), 2584-2590.

[35] Kearney K, Seo G, Matsushima T, Adachi C, Ertekin E, Rockett A. Computational Analysis of the Interplay between Deep Level Traps and Perovskite Solar Cell Efficiency. J Am Chem Soc 2018;140(46):15655–60

[36] Joshi P, Zhang L, Kottokkaran R, Abbas H, Hossain I, Nehra S, et al., editors. Physics of instability of perovskite solar cells. 2016 IEEE 43rd Photovoltaic Specialists Conference (PVSC); 2016 5-10 June 2016

[37] Joshi PH, Zhang L, Hossain IM, Abbas HA, Kottokkaran R, Nehra SP, et al. The physics of photon induced degradation of perovskite solar cells. AIP Adv 2016;6(11):115114.

[38] Yin W-J, Shi T, Yan Y. Unique Properties of Halide Perovskites as Possible Origins of the Superior Solar Cell Performance. Adv Mater 2014;26(27):4653–8.

[39] Adinolfi V, Yuan M, Comin R, Thibau ES, Shi D, Saidaminov MI, et al. The In-Gap Electronic State Spectrum of Methylammonium Lead Iodide Single-Crystal Perovskites. Adv Mater 2016;28(17):3406–10.

[40] de Quilettes DW, Vorpahl SM, Stranks SD, Nagaoka H, Eperon GE, Ziffer ME, et al. Impact of microstructure on local carrier lifetime in perovskite solar cells. Science 2015;348(6235):683–

[41] Leijtens T, Eperon GE, Barker AJ, Grancini G, Zhang W, Ball JM, et al. Carrier trapping and recombination: the role of defect physics in enhancing the open circuit voltage of metal halide perovskite solar cells. Energy Environ Sci 2016;9(11):3472–81.

[42] Heo S, Seo G, Lee Y, Lee D, Seol M, Lee J, et al. Deep level trapped defect analysis in CH3NH3PbI3 perovskite solar cells by deep level transient spectroscopy. Energy Environ Sci 2017;10(5):1128–33.

[43] Decock, K., Khelifi, S., Burgelman, M., 2011. Modelling multivalent defects in thin film solar cells. Thin Solid Films 519 (21), 7481–7484.

[44] Burgelman, M., Nollet, P., Degrave, S., 2000. Modelling polycrystalline semiconductor solar cells. Thin Solid Films 361-362, 527–532.

[45] Burgelman, M., Verschraegen, J., Degrave, S., Nollet, P., 2004. Modeling thin-film PV devices. Prog. Photovoltaics Res. Appl. 12 (23), 143–153.

[46] Verschraegen, J., Burgelman, M., 2007. Numerical modeling of intra-band tunneling for heterojunction solar cells in SCAPS. Thin Solid Films 515 (15), 6276–6279

[47] Mathur, A. and Singh, B. (2022). Computational Approach for Synthesis of Perovskite Solar Cells. In Perovskite Materials for Energy and Environmental Applications (eds K. Ahmad and W. Raza). https://doi.org/10.1002/9781119763376.ch1

[48] A.S. Mathur, Prem Pratap Singh, Sachin Upadhyay, Neetika Yadav, K.S. Singh, Digpratap Singh, B.P. Singh, Role of absorber and buffer layer thickness on Cu2O/TiO2 heterojunction solar cells, Solar Energy, 233, 287–291, (2022) https://doi.org/10.1016/j.solener.2022.01.047

[49] Bharti Sharma, A.S. Mathur, V.K. Rajput, I.K.Singh, B.P.Singh, Device modeling of non-fullerene organic solar cell by incorporating CuSCN as a hole transport layer using SCAPS, Optik, 251, 168457 (2022) https://doi.org/10.1016/j.ijleo.2021.168457

[50] A.S. Mathur, Sachin Upadhyay, Prem Pratap Singh, Bharti Sharma, Prateek Arora, Vikas Kumar Rajput, Purushottam Kumar, Digpratap Singh, B.P. Singh, Role of defect density in absorber layer of ternary chalcogenide Cu2SnS3 solar cell, Optical Materials 119, 11314 (2021) doi: https://doi.org/10.1016/j.optmat.2021.111314

[51] AS Mathur, BP Singh, Study of effect of defects on CdS/CdTe heterojunction solar cell, Optik 212, 164717 (2020), doi: https://doi.org/10.1016/j.ijleo.2020.164717

[52] Arpit Swarup Mathur, Shalini Dubey, Nidhi, BP Singh, Study of role of different defects on the performance of CZTSe solar cells using SCAPS, Optik, 206, 163245 (2020) doi: https://doi.org/10.1016/j.ijleo.2019.163245

[53] Ahirrao, P. B., Gosavi, S. R., Sonawane, S. S., & Patil, R. S. (2011). Wide band gap nanocrystalline CuSCN thin films deposited by modified chemical method. *Arch. Phys. Res*, *2*(3), 29-33.

[54] Anwar, F., Mahbub, R., Satter, S. S., & Ullah, S. M. (2017). Effect of different HTM layers and electrical parameters on ZnO nanorod-based lead-free perovskite solar cell for high-efficiency performance. *International Journal of Photoenergy*, *2017*.

[55] Baumann, A., Lorrmann, J., Deibel, C., & Dyakonov, V. (2008). Bipolar charge transport in poly (3-hexyl thiophene)/methanofullerene blends: A ratio dependent study. *Applied Physics Letters*, *93*(25), 252104.

[56] Behrouznejad, F., Shahbazi, S., Taghavinia, N., Wu, H. P., & Diau, E. W. G. (2016). A study on utilizing different metals as the back contact of CH 3 NH 3 PbI 3 perovskite solar cells. *Journal of Materials chemistry A*, *4*(35), 13488-13498.

[57] Fabregat-Santiago, F., Randriamahazaka, H., Zaban, A., Garcia-Canadas, J., Garcia-Belmonte, G., & Bisquert, J. (2006). Chemical capacitance of nanoporous-nanocrystalline TiO 2 in a room temperature ionic liquid. *Physical Chemistry Chemical Physics*, *8*(15), 1827-1833.

[58] Hussain, A., Ahmed, R., Ali, N., Butt, F. K., Shaari, A., Shamsuri, W. W., ... & Verma, K. D. (2016). Post annealing effects on structural, optical and electrical properties of CuSbS2 thin films fabricated by combinatorial thermal evaporation technique. *Superlattices and Microstructures*, *89*, 136-144.

[59] Khaliq, A., Xue, F. L., & Varahramyan, K. (2009). Numerical simulation of spin coated P3HT organic thin film transistors with field dependent mobility and distributed contact resistance. *Microelectronic engineering*, *86*(11), 2312-2315.

[60] Laban, W. A., & Etgar, L. (2013). Depleted hole conductor-free lead halide iodide heterojunction solar cells. *Energy & Environmental Science*, *6*(11), 3249-3253.

[61] Liu, D., & Kelly, T. L. (2014). Perovskite solar cells with a planar heterojunction structure prepared using room-temperature solution processing techniques. *Nature photonics*, *8*(2), 133-138.

[62] Liu, F., Zhu, J., Wei, J., Li, Y., Lv, M., Yang, S., ... & Dai, S. (2014). Numerical simulation: toward the design of high-efficiency planar perovskite solar cells. *Applied Physics Letters*, *104*(25), 253508.

[63] Poplavskyy, D., & Nelson, J. (2003). Nondispersive hole transport in amorphous films of methoxy-spirofluorene-arylamine organic compound. *Journal of Applied Physics*, *93*(1), 341-346.

[64] Stoumpos, C. C., Malliakas, C. D., & Kanatzidis, M. G. (2013). Semiconducting tin and lead iodide perovskites with organic cations: phase transitions, high mobilities, and near-infrared photoluminescent properties. *Inorganic chemistry*, *52*(15), 9019-9038.

[65] Teimouri, R., & Mohammadpour, R. (2018). Potential application of CuSbS2 as the hole transport material in perovskite solar cell: a simulation study. *Superlattices and Microstructures*, *118*, 116-122.

[66] Wang, M., Zang, Z., Yang, B., Hu, X., Sun, K., & Sun, L. (2018). Performance improvement of perovskite solar cells through enhanced hole extraction: the role of iodide concentration gradient. *Solar Energy Materials and Solar Cells*, *185*, 117-123.

[67] Raoui, Y., Ez-Zahraouy, H., Tahiri, N., El Bounagui, O., Ahmad, S., & Kazim, S. (2019). Performance analysis of MAPbI3 based perovskite solar cells employing diverse charge selective contacts: Simulation study. *Solar Energy*, *193*, 948-955.

[68] Yang, K. J., Kim, S., Sim, J. H., Son, D. H., Kim, D. H., Kim, J., ... & Kang, J. K. (2018). The alterations of carrier separation in kesterite solar cells. *Nano Energy*, *52*, 38-53.

[69] DeQuilettes, D. W., Zhang, W., Burlakov, V. M., Graham, D. J., Leijtens, T., Osherov, A., ... & Stranks, S. D. (2016). Photo-induced halide redistribution in organic–inorganic perovskite films. *Nature communications*, *7*(1), 1-9.

[70] de Quilettes, D. W., Vorpahl, S. M., Stranks, S. D., Nagaoka, H., Eperon, G. E., Ziffer, M. E., ... & Ginger, D. S. (2015). Impact of microstructure on local carrier lifetime in perovskite solar cells. *Science*, *348*(6235), 683-686.

[71] Leblebici, S. Y., Leppert, L., Li, Y., Reyes-Lillo, S. E., Wickenburg, S., Wong, E., ... & Weber-Bargioni, A. (2016). Facet-dependent photovoltaic efficiency variations in single grains of hybrid halide perovskite. *Nature Energy*, *1*(8), 1-7.

[72] Cao, J., Wu, B., Chen, R., Wu, Y., Hui, Y., Mao, B. W., & Zheng, N. (2018). Efficient, hysteresis-free, and stable perovskite solar cells with ZnO as electron-transport layer: effect of surface passivation. *Advanced Materials*, *30*(11), 1705596.

[73] Futscher, M. H., Lee, J. M., McGovern, L., Muscarella, L. A., Wang, T., Haider, M. I., ... & Ehrler, B. (2019). Quantification of ion migration in CH 3 NH 3 PbI 3 perovskite solar cells by transient capacitance measurements. *Materials Horizons*, *6*(7), 1497-1503.

Cite this Article

Prem Pratap Singh and Kripa Shanker Singh, "Investigation via simulation of the influence of defects on the photovoltaic performance of single-junction perovskite solar cells based on $MAPbI_3$ using SCAPS-1D", *International Journal of Multidisciplinary Research in Arts, Science and Technology (IJMRAST), ISSN: 2584-0231, Volume 1, Issue 5, pp. 37-47, December 2023.*

Journal URL: *https://ijmrast.com/*